

<https://doi.org/10.1038/s41545-024-00332-7>

# Investigation of scaling inhibition and biofouling potential of different molecular weight fractions of a PAA antiscalant

Check for updates

S. A. Kaushik <sup>1,2</sup> ✉, D. Armbruster<sup>3</sup>, J. Dittmer<sup>1</sup>, D. Bruniecka-Sulewski<sup>2</sup>, B. Wendler<sup>2</sup> & M. Ernst <sup>1,2</sup> ✉

This study investigates the scale inhibition performance of a commercial polyacrylic acid-based (PAA) antiscalant used for drinking water production and its molecular weight fractions ( $\leq 500$  Da,  $\geq 500$  Da). The investigated antiscalant is used to prevent sulfate and carbonate scaling in treatment of drinking water sources by reverse osmosis or nanofiltration (RO/NF). Based on two complementary tests involving determination of induction time in a batch test and rate of flux decline in a lab-scale RO/NF plant, concordant results were obtained, proving that the overall performance of commercial PAA was controlled almost entirely by the higher molecular weight fraction. The low molecular weight fraction, which is potentially more permeable through the NF/RO membrane, showed poor inhibition against both sulfate and carbonate scalants. Furthermore, measurements on the assimilable organic carbon (AOC) by flow cytometry reveals that the low molecular weight PAA fraction has low biological stability, as its potential transport into the permeate of a NF270 nanofiltration membrane was inferred by elevated AOC values in the NF-permeate. These results are crucial information for water utilities, plant engineering, regulatory bodies and public authorities with respect to the possible operation of RO/NF especially in drinking water production.

High-pressure membrane filtration using nanofiltration or reverse osmosis can be used for treatment of freshwater sources to remove divalent and/or monovalent ions, trace organics and anthropogenic micropollutants in advanced drinking water treatment. RO membrane systems typically operate with feed pressures in the 10–85 bar range and became the dominant technology for seawater desalination across the world<sup>1</sup>. Though NF/RO are established technologies for water treatment, the problem of membrane scaling at elevated water recoveries remains persistent<sup>2</sup>. When the concentration of inorganics exceeds their solubility limit, due to concentration polarization, salts may precipitate on the membrane surface leading to a rapid decline in performance and potential membrane destruction. The scale may form dense layers resulting in high hydraulic resistance and a significant reduction in permeability of the membrane.

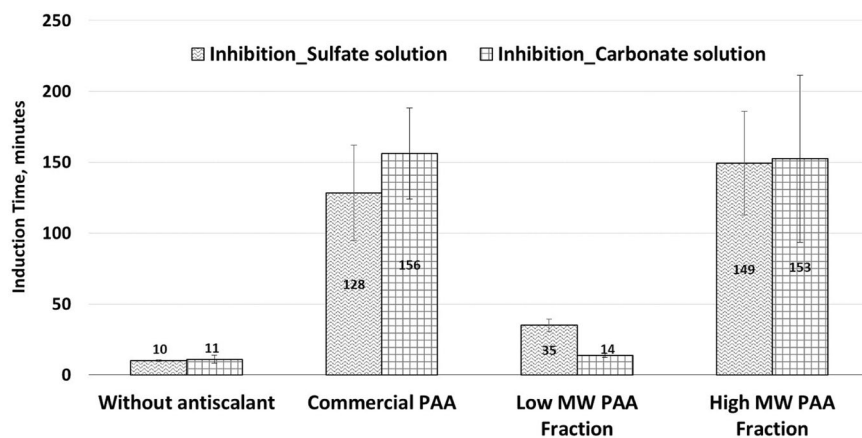
To mitigate the risk of membrane scaling, many methods, including feed water pre-treatment, the adaptation of operational parameters, the development of novel membrane materials and innovation in feed spacers have been researched<sup>3</sup>. However, the current most reliable method used to control scaling in NF/RO involves the addition of antiscalants. These

typically comprise of chemical formulations that can retard and/or inhibit scale formation through a single or combination of scale inhibition mechanisms. Discussed examples are the delay of nucleation and crystallization stages through inhibition mechanisms such as chelation, dispersion, lattice distortion, complexation and threshold effect, which have previously been widely hypothesized<sup>4</sup>. Antiscalants are commonly known to contain chemical agents with various functional groups such as phosphonic, carboxylic, and sulfonic acid groups which interact with the scalants<sup>5</sup>.

While commercial antiscalants were initially phosphorus (P)-based, research into the suitability of P-free antiscalants is widely pursued, primarily due to environmental concerns with phosphorus emissions linked to eutrophication potential when brines are discharged into receiving waters<sup>4</sup>. Polycarboxylic and polyacrylic acids (PAA) based antiscalants are one of the most common alternatives developed and sometimes even advocated as environment-friendly antiscalants due to lack of phosphorus<sup>2,4,6</sup>. Besides the type of functional groups present within the polymeric antiscalant, molecular size, and conformation of polymers due to their distinct long-chain structural features are particularly important to

<sup>1</sup>Institute of Water Resources and Water Supply, Hamburg University of Technology, Am Schwarzenberg-Campus 3, 21073 Hamburg, Germany. <sup>2</sup>DVGW-Forschungsstelle TUHH, Am Schwarzenberg-Campus 3, 21073 Hamburg, Germany. <sup>3</sup>TZW: DVGW-Technologiezentrum Wasser, Karlsruher Str. 84, 76139 Karlsruhe, Germany. ✉e-mail: [shambhavi.kaushik@tuhh.de](mailto:shambhavi.kaushik@tuhh.de); [mathias.ernst@tuhh.de](mailto:mathias.ernst@tuhh.de)

**Fig. 1 | Induction time of antiscalants using the stirred beaker test.** Induction time (based on 1 NTU turbidity increase<sup>20,21</sup>) with 0.5 mg TOC L<sup>-1</sup> of commercial PAA and its low and high MW fractions, against 68 mM sulfate solution and 33 mM carbonate solution (T = 11 °C, SI<sub>CaSO<sub>4</sub></sub> = 0.72, SI<sub>CaCO<sub>3</sub></sub> = 2.06). Error bars indicate standard deviation from duplicate experimental sample measurements.



determine the efficacy of the product<sup>2,5</sup>. It has been established that molecular weight (MW) of the polymer is a crucial parameter influencing the overall scale inhibition potential of the antiscalant<sup>2,6–9</sup>. PAA antiscalants of different MWs have been found to exhibit varying inhibition characteristics, such as acting as a threshold agent within a MW range of 1000–3000 Da, exhibiting lattice distortion effect at a MW range of 5000–10,000 Da, and working as a dispersion agent at an MW range of 20,000–40,000 Da<sup>7</sup>. However, some studies indicated that polymeric antiscalants with extremely high MW or when overdosed could result in poor inhibition performance, probably due to their bridging flocculation effects<sup>9–11</sup>. Shen et al.<sup>8</sup>, investigated scale inhibition by different molecular weights of PAA against calcium carbonate and derived that 2500–7000 Da is suitable for PAA antiscalants to inhibit calcium carbonate scaling, apparently in the range of a commercial product<sup>8</sup>. Additionally, they showed that application of a PAA with an average molecular weight above 2500 Da resulted in lower binding energy between salts and antiscalants, thus leading to earlier carbonate clusters. From a dosage of 1.5 mg L<sup>-1</sup> onwards, the inhibition ratio curves (calculated based on change in calcium concentration in solution) of all PAA followed the same pattern, whereas below this value, scale inhibition potential was attenuated for PAAs with larger molecular weight above 2500 Da<sup>8</sup>.

The use of P-based antiscalants has been receiving considerable attention from regulatory authorities to limit their usage due to environmental concerns. PAA-based antiscalants are increasingly being recommended as a good alternative to the P-based products. However, due to proprietary reasons and the challenges of low concentration polymer analysis, there is still limited information on the different components of these products, their effectiveness and consequences. Based on the production process and/or the manufacturer, commercial PAA antiscalants may contain varying molecular weights distributions, which remain unknown to users. This study delved into the scale inhibition effectiveness of a commonly used commercial PAA antiscalant and its different molecular weight fractions. The antiscalants' effectiveness was investigated by two methods: a simple batch configuration and a crossflow operated membrane filtration setup. It is revealed that the inhibition effect of PAA strongly depends on the molecular weight and that the low molecular weight fraction is of specific significance as it barely contributes to the scaling inhibition and at the same time shows higher biological growth potential.

## Results and discussion

### Effectiveness of PAA fractions in the Stirred Beaker Test

To compare the performance of the commercial PAA antiscalant as well as the two fractions, an identical TOC concentration of 0.5 mg L<sup>-1</sup> each was dosed. The antiscalants were first evaluated for their inhibition potential against CaSO<sub>4</sub> and CaCO<sub>3</sub> scaling via the induction time using the batch stirred beaker test, with three experimental replicates. As seen in Fig. 1, in the absence of an antiscalant, supersaturated sulfate and carbonate solutions have an induction time of only about 10 min. Adding 0.5 mg TOC L<sup>-1</sup> of the

commercial PAA antiscalant caused a significant increase in the induction time for both salts (130 min to 155 min). Interestingly, the investigation of the fractions clearly showed that the low MW fraction (≤ 500 Da) led to a very low induction time for sulfate and carbonate scalants (35 min and 14 min, respectively). In contrast, the high MW fraction led to high induction times for both scaling salts, comparable to the commercial PAA product.

Since it can be expected that higher induction times correlate to a better performing antiscalant, these results imply that the performance of the commercial PAA is mainly controlled by the large MW fraction (≥ 500 Da). This information is largely in agreement to several earlier studies reporting effective scale inhibition performance by PAAs in the range of 2000 Da to 7000 Da and 100,000 Da against calcium sulfate and calcium carbonate, as summarized in Table 1<sup>6,8,12</sup>. The molecular PAA weights covered by these studies were above the low molecular weight PAA fraction investigated in the present study (≤ 500 Da). To our knowledge, the effectiveness of PAAs ≤ 500 Da has not been previously investigated, whereas the molecular weight distributions of commercial antiscalants are not disclosed by the manufacturers.

The induction times derived from stirred-beaker tests at elevated concentrations of sparingly soluble salts are often associated with high standard deviations. Lab-scale RO pilot plant experiments were performed to cross-verify the outcomes of the inhibition performance.

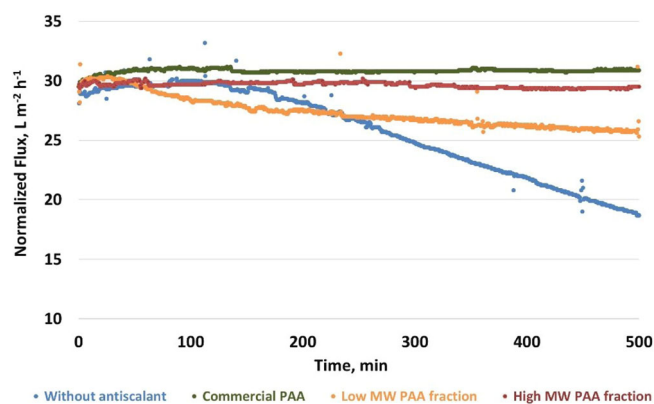
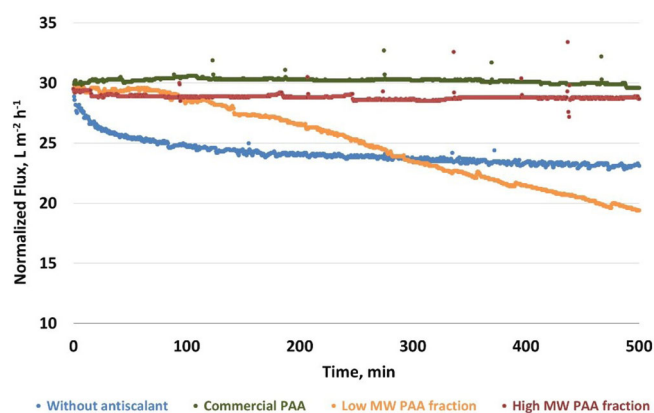
### Effectiveness of PAA fractions in lab-scale RO experiments

To verify the inhibition effectiveness observed during the batch setup, an identical antiscalant dosage of 0.5 mg TOC L<sup>-1</sup> was used. As seen in Fig. 2, when tested at constant TMP of 25 bar against 25 mM sulfate feed, application of the low MW PAA fraction led to a continuous decrease in flux. Almost 15% decline was recorded after 200 min, comparable to the blank experiment without any antiscalant, indicating low gypsum scale inhibition potential. After 200 min, the blank flux further decreased at a linear rate whereas the flux of the experiment with the low MW fraction decreased at an attenuated rate. In contrast, application of the commercial product as well as its high MW fraction was able to maintain a relatively constant and comparable flux throughout the experiment (500 min), thus confirming effective scale inhibition against gypsum. Comparable inhibition performance results were observed with 22 mM carbonate solutions (Fig. 3), with the low MW fraction showing poor calcite inhibition when compared to the high MW fraction and the commercial product.

Al-Hamzah et al.<sup>13</sup> studied the calcium carbonate scale inhibition efficiency of PAAs with different average molar masses (determined using <sup>1</sup>H-NMR spectroscopy and Gel Permeation Chromatography), synthesized by Atomic Transfer Radical Polymerization (ATRP) and containing different end groups. They report that, at room temperature, PAA polymers with average molar masses between 1000–3000 Da, containing short (carboxymethyl-1,1-dimethyl-PAA & ethyl-isobutyrate-PAA) to moderately

**Table 1 | Comparison of different molecular weights of PAA antiscalants and their corresponding scale inhibition effectiveness according to cited studies and the present study**

Parameter to evaluate antiscalant effectiveness	Molecular weight of PAA reported	Effectiveness of respective PAA against CaSO <sub>4</sub> /CaCO <sub>3</sub> scaling	Study
Induction time based on turbidity increase of 1 NTU	≤500 Da	Low/nil inhibition of both CaSO <sub>4</sub> and CaCO <sub>3</sub> scaling	Current study
	≥500 Da	High CaSO <sub>4</sub> and CaCO <sub>3</sub> inhibition	
Inhibition efficiency via change in Ca <sup>2+</sup> concentration	2500–7000 Da	Effective CaCO <sub>3</sub> inhibition by PAA with MW 2500 Da; no enhanced inhibition by PAA with higher MW	Shen et al. <sup>8</sup>
Induction time via slope of turbidity (0–100%) vs. time (0–300 min) plots	2000 Da	10% turbidity increase in ~200 min against CaSO <sub>4</sub>	Rabizadeh et al. <sup>12</sup>
	100,000 Da	10% turbidity increase in ~50 min against CaSO <sub>4</sub>	
Inhibition efficiency via change in Ca <sup>2+</sup> concentration	6043 Da	Good CaCO <sub>3</sub> inhibition reported for given PAA compared to other antiscalants	Zuo et al. <sup>6</sup>

**Fig. 2 | Flux behavior in the lab-scale RO experiments during gypsum scaling.** Flat sheet RO membrane operated with 25 mM Na<sub>2</sub>SO<sub>4</sub> and CaCl<sub>2</sub> feed and commercial PAA and its low and high MW fractions (Antiscalant dosing as 0.5 mg TOC L<sup>-1</sup> in each experiment); TMP = 25 bar, complete recirculation mode, T = 11 °C, SI<sub>gypsum</sub> ≈ 0.2.**Fig. 3 | Flux behavior in the lab-scale RO experiments during calcite scaling.** Flat sheet RO membrane operated with 22 mM NaHCO<sub>3</sub> and CaCl<sub>2</sub> feed and commercial PAA and its low and high MW fractions (Antiscalant dosing as 0.5 mg TOC L<sup>-1</sup> in each experiment); TMP = 25 bar, complete recirculation mode, T = 11 °C, SI<sub>calcite</sub> ≈ 1.09.

sized (cyclohexyl-isobutyrate-PAA & *N*-hexyl-isobutyrate-PAA) end groups, provide good inhibition against carbonate scaling. In comparison to that, dosing of larger PAA polymers (approx. >9000 Da) failed in being effective against scale prevention. The molecular weight distribution of the commercial PAA antiscalant has been characterized by Armbruster et al.<sup>14</sup> An average molecular weight of ≤1200 Da was determined. PAA molecules of up to 7000 Da were detected, yet with their relative contribution rapidly

decreasing from the average molecular weight onwards. Thus, the high MW fraction of the commercial PAA (≥500 Da) used in this study lies in a comparable range as the molecular weight range determined as suitable for effective scaling inhibition by Al-Hamzah et al.<sup>13</sup>, whereas the low MW fraction investigated (≤500 Da) in the present study clearly falls below it. The pilot plant tests using the crossflow cell confirmed the inhibition and performance results obtained from the batch stirred beaker test for both gypsum and calcite.

### SEM characterization of the membranes

The membranes tested in the lab-scale plant were then characterized by SEM analysis to identify the crystal behavior and formation of gypsum and carbonate salts. Similar to the scale inhibition trends observed in the pilot plant, it was seen that the membranes operated with the low MW fraction of the antiscalant showed several gypsum and calcite crystals on their surfaces (Figs. 4c and 5c), similar to the membranes that were scaled without antiscalants (Figs. 4a and 5a), although of a slightly different size and morphology. Differences in the size and morphology of the crystals are believed to be responsible for the respective flux decline for the two scalants. Deformed gypsum crystals in the presence of low MW PAA fraction leads to faster flux decline compared to blank in the beginning, but at an attenuated rate after 200 min (Figs. 2 and 4c). Blank calcite crystals being smaller and denser lead to faster initial flux decline, while the low MW PAA which forms larger calcite crystals, leads to slower flux decline in the beginning, but becomes more rapid after 300 min (Figs. 3 and 5c). As seen in Figs. 4d and 5d, the membranes operated with the high MW fraction of the PAA were the cleanest of all experiments, closely followed by the membrane operated with the commercial PAA product (Figs. 4b and 5b), thus proving again that the lower MW fractions of the commercial PAA product have little to no contribution on the overall scale inhibition potential of the antiscalant.

### Biological stability of water after dosing PAA

Biofouling in NF/RO systems is a relevant topic investigated in numerous studies<sup>15–17</sup>. The primary focus of the cited studies was on (i) biofouling caused by water constituents, (ii) the applied antiscalants, (iii) methods for detection and (iv) strategies to mitigate scaling. Sweity et al.<sup>17</sup> revealed that biofouling within the RO system can also be initiated or promoted by antiscalants dosed during treatment, with a particular biofouling potential pointed out for PAA based agents. Vrouwenvelde et al.<sup>16</sup> recommended AOC measurements for the rapid screening of biofouling potential.

In order to verify this accordingly, tests on the biological stability of the two molecular weight fractions and the commercial PAA product itself were conducted, based on likewise TOC dosage of 1 mg L<sup>-1</sup>. The antiscalant samples were prepared in Hamburg tap water (TOC ≈ 0.5 mg L<sup>-1</sup>), providing an initial bacterial concentration of about 34,700 Cells mL<sup>-1</sup>. The total cell count measurements were performed over a 28-day duration at regular measuring intervals. The flow cytometry data shown in Fig. 6 was converted to AOC values as shown in Table 2.



**Fig. 4 | SEM images of RO membrane surface after gypsum scaling experiments.** RO membrane surface after operation with 25 mM  $\text{Na}_2\text{SO}_4$  and  $\text{CaCl}_2 + 0.5 \text{ mg TOC L}^{-1}$  of PAA antiscalant and its low and high MW fractions. **a** Without antiscalant, **b** commercial PAA, **c** low MW PAA, **d** High MW PAA; (Magnification = 500 $\times$ ; 20  $\mu\text{m}$ ).

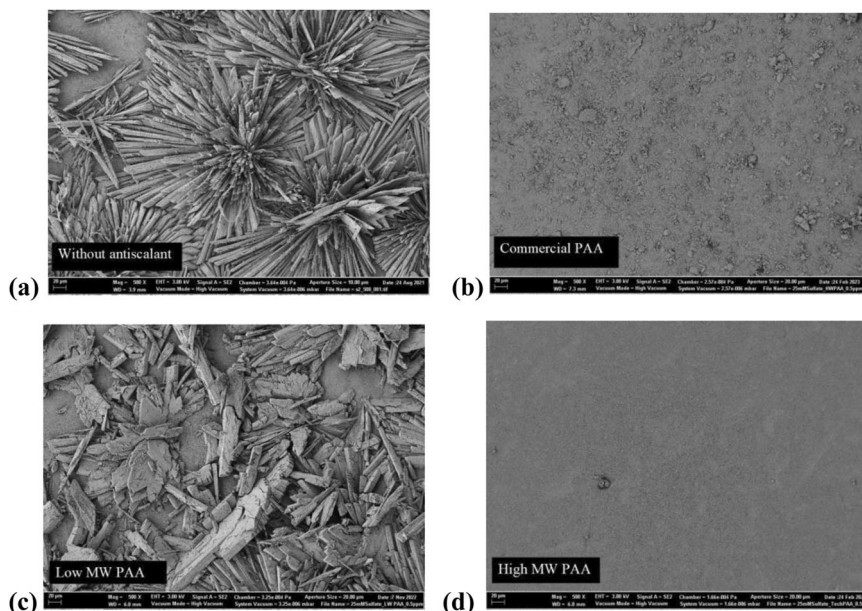
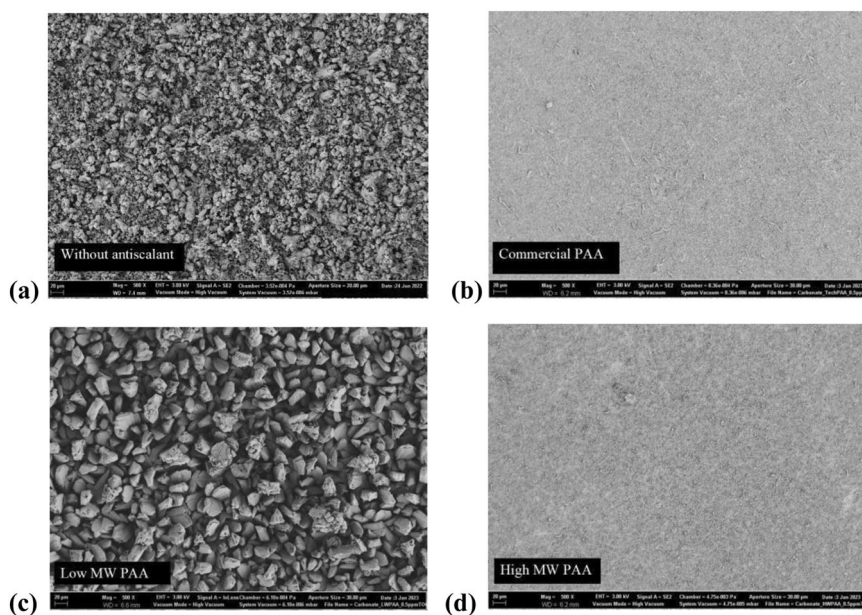


**Fig. 5 | SEM images of RO membrane surface after calcite scaling experiments.** RO membrane surface after operation with 22 mM  $\text{NaHCO}_3$  and  $\text{CaCl}_2 + 0.5 \text{ mg TOC L}^{-1}$  of PAA antiscalant and its low and high MW fractions. **a** Without antiscalant, **b** commercial PAA, **c** low MW PAA, **d** High MW PAA; (Magnification = 500 $\times$ ; 20  $\mu\text{m}$ ).



Tap water maintained most stable and had the lowest AOC over the entire 28-day range and the high MW fraction led to comparable results. The commercial product showed a similar trend as tap water but with a slightly enhanced AOC value. The low MW fraction, in contrast, led to a significantly increased AOC over the entire 28-day range, implying that the PAA constituents of low MW are readily bioavailable to bacteria and susceptible to enhance the biofouling potential.

The biological stability of the PAA's organic carbon is of particular concern with respect to the possibility of transfer of the small PAA molecules into the permeate. Therefore, AOC measurements of the permeate arising from a NF membrane (NF270) filtration with tap water feed and dosage of  $1 \text{ mg TOC L}^{-1}$  commercial PAA (equivalent to approx.  $10 \text{ mg L}^{-1}$  of liquid AS product) and its low and high MW fractions were performed. The NF permeates operated with the commercial PAA product and its low MW fraction showed slightly enhanced biological growth (>25% more) as compared to the permeate derived from application of the high molecular weight fraction (Supplementary Fig. 4 and Supplementary Table 1). Due to

the stabilization of the NF process during prolonged running times, this trend became more obvious after 14 days (Supplementary Discussion 1).

These results are in agreement with previous observations of increased biofouling and degradation of RO membranes operated with PAA-based antiscalants<sup>18,19</sup>. Sweity et al.<sup>18</sup> found that PAA-based antiscalants alter the physico-chemical properties of thin film composite RO membranes, e.g. increased hydrophobicity and surface charge, rendering them more susceptible for the deposition and attachment of bacterial cells. Ashfaq et al.<sup>19</sup> also suggested that PAA-based antiscalants contribute to biofouling on membranes and focused on devising a biofouling screening method for antiscalants using FTIR multivariate analysis and principle component analysis (PCA) with colony forming unit (CFU) counts.

The current study supports these earlier findings with regard to enhanced biofouling potential on membranes operated with PAA-based antiscalants. Additionally, indications were derived that the application of PAA-based antiscalants may be associated with enhanced AOC levels in the permeate due to potential permeability of small antiscalant molecules.

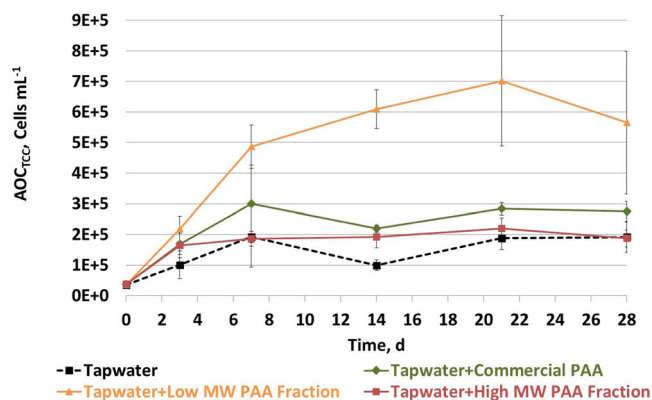


**Fig. 6 | Biological stability of antiscalants via flow cytometry.** Total cell count (TCC) values of commercial PAA and its low and high MW fractions (1 mg TOC L<sup>-1</sup>) conducted in Hamburg tap water using flow cytometer. Error bars indicate standard deviation from triplicate sample measurements.

**Table 2 | Assimilable organic carbon (AOC) values of commercial PAA, its low and high MW fractions (each 1 mg TOC L<sup>-1</sup>) conducted in Hamburg tap water, determined by flow cytometer via total cell counts**

Sample label	AOC, $\mu\text{g C}_{\text{eq}} \text{L}^{-1}$
Tapwater	15.7 ± 9.9
Tapwater + Commercial PAA (1 mg TOC L <sup>-1</sup> )	26.2 ± 12.6
Tapwater + Low MW Fraction (1 mg TOC L <sup>-1</sup> )	66.6 ± 21.3
Tapwater + High MW Fraction (1 mg TOC L <sup>-1</sup> )	18.2 ± 3.5

## Discussion

The use of PAA-based antiscalants as an alternative to phosphonate-based products has garnered increased attention recently, as public authorities tend to promote the application of P-free chemicals to prevent eutrophication in receiving waters. While the scale inhibition effectiveness may be sufficient, it has been determined that a commonly used commercial PAA antiscalant product contains significant amounts (~27% contribution to the TOC) of low molecular weight polyacrylic acid polymers ( $\leq 500$  Da). Based on two kinds of complementary experimental test methods and subsequent membrane characterization, it was shown that the inhibition of gypsum and calcite is mainly linked to the high MW fraction ( $\geq 500$  Da) within the investigated PAA. In contrast, the low MW fraction of the PAA antiscalant shows low to nil scale inhibition potential for the two salts in the batch and small-scale pilot tests. Moreover, AOC measurements based on TCC demonstrate that the PAA's low MW fraction exhibits enhanced biological growth potential (lower biological stability) compared to the high MW fraction, potentially facilitating biofouling on the membranes surface. Having investigated solely one commonly used commercial PAA antiscalant, the authors acknowledge that different manufacturers and/or different production processes may influence the proportion of low MW PAA constituents as well as the overall molecular weight distribution of the resulting PAA product. Nonetheless, the observation that present low MW PAA constituents ( $\leq 500$  Da) are affiliated with enhanced biofouling potential is crucial for the operation of membrane plants. Indications for enhanced membrane permeability through less-dense RO/NF membranes (if, for example, hardness reduction is the targeted treatment objective) were derived by measuring the AOC of the NF permeate operated with the commercial antiscalant as well as the low MW PAA fraction. Consequently, permeates with enhanced biological growth potential may result, which is of particular concern for the production of potable water from groundwater, especially if the product water is not disinfected (like often the case in Germany and Scandinavian countries).

## Methods

### Antiscalant and salt solutions

A commercial PAA based antiscalant and its high and low molecular weight fractions were used to investigate the effectiveness on scale inhibition. For accurate dosing, a 0.1% to 1% (by weight) stock solution of the antiscalant was prepared and used within 24 h. The effectiveness of the antiscalant was tested against CaSO<sub>4</sub> and CaCO<sub>3</sub> scalants. To achieve supersaturated concentrations of the two salts, a mixture of different amounts of Na<sub>2</sub>SO<sub>4</sub> with CaCl<sub>2</sub> (Carl Roth GmbH) and NaHCO<sub>3</sub> with CaCl<sub>2</sub> (Carl Roth GmbH) were respectively used. Stock solutions of the order of 50 g L<sup>-1</sup> of Na<sub>2</sub>SO<sub>4</sub>, 20 g L<sup>-1</sup> of NaHCO<sub>3</sub> and 50 g L<sup>-1</sup> CaCl<sub>2</sub> were used for all experiments and stored in the refrigerator for a maximum of 3 days; NaHCO<sub>3</sub> was freshly prepared before each experiment. All salt stock solutions were filtered through a 0.1  $\mu\text{m}$  cellulose nitrate filter to remove undissolved particles that may trigger crystal nuclei formation and negatively impact reproducibility of results. The pH of the stock solutions was adjusted to 7.5 using 0.1 mol L<sup>-1</sup> or 1 mol L<sup>-1</sup> HCl and 0.1 mol L<sup>-1</sup> NaOH, if required.

Ultrapure water used for solution preparation and cleaning was obtained from 'Millipore Direct-Q 5 UV System' (Merck, Darmstadt, Germany), with the water output having an electrical resistivity of 0.056  $\mu\text{S cm}^{-1}$  (at 25 °C) and total organic carbon (TOC) concentration  $< 5 \mu\text{g L}^{-1}$ . The water passes a built-in photooxidation UV lamp before leaving the device. Purification cartridges were replaced as recommended by the manufacturer.

### Fractioning of the antiscalant

The fractioning of the commercial PAA antiscalant into large and small molecular weight fractions was carried out by mixing 250 ml of commercial PAA antiscalant with 50 ml of 2 mol L<sup>-1</sup> NaOH and 200 ml of methanol (MeOH). Solutions were shaken and stored at  $-20$  °C until phase separation. During this process, the long-chain polymers separated out as a viscous brownish mass at the bottom, while the short-chain polymers dissolved in the supernatant. After separation of the supernatant, the viscous fraction was extracted two more times with MeOH, during which viscosity increased. The extracts were combined and evaporated at 100 mbar and 35 °C. After the MeOH had largely distilled over and the vacuum pressure remained constant, evaporation was continued for six hours at 50 mbar and 40 °C in order to remove traces of MeOH. The aqueous and viscous high molecular weight fraction was diluted with 50 mL of Milli-Q ultrapure water (MQ) and likewise stripped off residual MeOH for six hours at 50 mbar and 40 °C. The volume of both the fractions was then made up with MQ water to the initial volume of the commercial PAA. Alkaline hydrolysis is expected to play a minor role in the handling of polyacrylic acids due to aliphatic linkage of the acrylic acid units and unsubstituted carboxy groups (in contrast to e.g., polyacrylic amides or polyacrylic esters). In fact, the commercial PAA-antiscalants are commonly supplied as partially neutralized sodium salt with slightly alkaline pH. The antiscalant investigated in the current study had pH 8. No notable change was observed with IC-ESI-QTOF analysis after prolonged storage ( $\geq 4$  weeks) of the derived PAA fractions.

Based on this fractionation and a PAA analysis method developed by TZW, Karlsruhe (described under Supplementary Method 1 and Armbruster et al.<sup>14</sup>), the low MW fraction predominantly contained PAA molecules in a molecular weight range of  $\leq 500$  Da, while the high MW fraction predominantly covered the molecular weight range of  $\geq 500$  Da.

### Antiscalant characterization (TOC/DOC and LC-OCD)

The TOC/DOC of the commercial PAA antiscalant and its fractions were determined using the Shimadzu TOC-V CSM total organic carbon analyzer. Triplicate samples were used for the analysis, with the device performing 5 measurements per sample. The commercial antiscalant is comprised of a mixture of PAA molecules with varying chain lengths, i.e. molecular weights, which were fractionated into two molecular weight fractions of  $\leq 500$  Da and  $\geq 500$  Da. However, the fractions still represent non-uniform mixtures of PAA molecules with their molecular weight distribution shifted to either the high or the low end of the initial distribution within the

commercial product. While the low molecular fraction contains a large number of smaller molecules, the large molecular fraction contains a comparatively small number of larger molecules. The determination of the molar concentration of a polymeric mixture is nontrivial. Concurrently, the comparison according to substance concentration, e.g. via dry weight, would not reflect the molar constitution. In order to experimentally compare the three PAA solutions, standardization according to DOC measurements was performed. As the PAA molecules primarily consist of polyacrylic acid chains with repeating  $[-CH_2-CH(COOH)-]$ -units, the DOC may be regarded as a function of the carboxyl group concentration. Carboxyl groups are the primary functional groups of PAAs and contribute to the antiscalant properties. Thus, it was decided to evaluate the effectiveness of the antiscalant and the derived fractions based on the DOC. Different concentrations between 1 and 20 mg L<sup>-1</sup> of the commercial PAA antiscalant and its two molecular weight fractions were prepared using the 0.1% stock solution (for ex. 1 mL L<sup>-1</sup> for the former concentration and 20 mL L<sup>-1</sup> for the latter dosage). Molecular weights of the commercial PAA product and its two fractions were characterized by size-exclusion chromatography coupled to organic carbon detection (LC-OCD) and UV-detection (UVD; 254 nm) (DOC-Labor Dr. Huber). This setup was also used to identify qualitative changes in DOC within the samples. ChromeRES and ChromeCALC by DOC-Labor Dr. Huber were used for data analyses and correction measures. The corresponding diagram derived from the analysis are given in Supplementary Figs. 2 and 3, correlated to the description in Supplementary Method 2 and Supplementary Method 3, respectively.

### Stirred beaker test

To determine the antiscalant effectiveness, a batch test adapted along the lines of the NACE Standard TM0374-2007 test and Benecke et al.<sup>20</sup> was used. It consisted of a 500 ml beaker containing supersaturated scaling solution and antiscalant at 11 ± 0.5 °C, which was magnetically stirred. The solution was protected from light and the turbidity of the solution was recorded every minute using the Multi 3630 IDS Multiparameter measuring device from Xylem Analytics Germany Sales GmbH & Co. KG, WTW. To determine the effectiveness of the antiscalant, induction time was defined as time taken for the turbidity of the solution to increase by 1 NTU<sup>20,21</sup>. After each experiment, the glass beaker was thoroughly washed and the electrodes cleaned by dipping in 0.5 M HCl for 30 min, followed by rinsing with MQ water. Each experimental trial with the stirred beaker test was carried out three times to determine the standard deviation and evaluate the reproducibility of the test.

### Lab-scale pilot plant test

A fully automated bench-scale RO setup developed at the Institute of Water Resources and Water Supply, TUHH and previously described by Benecke et al.<sup>20,21</sup> was used to verify the antiscalant performance results from the stirred beaker test. Flatsheet commercial RO membrane, CR100 and commercial NF membrane, NF270 both from DuPont were used for the experimental trials. The plant was operated at 11 ± 1 °C with 6 L of a slightly supersaturated sulfate (saturation index,  $SI_{\text{gypsum}} \approx 0.2$ ) or carbonate feed ( $SI_{\text{calcite}} \approx 1.09$ ), at constant transmembrane pressure (TMP) of 25 bar and 0.1 m s<sup>-1</sup> cross-flow velocity in complete recirculation mode (permeate + retentate recirculation) to maintain the saturation conditions within the system, thereby establishing that any decline in the flux is due to ineffectiveness of the antiscalant. The designated starting flux of 30 L m<sup>-2</sup> h<sup>-1</sup> deviated by about ±5 L m<sup>-2</sup> h<sup>-1</sup> in between experiments. For comparison of different trials, the initial fluxes were normalized to an initial value of 29.5 L m<sup>-2</sup> h<sup>-1</sup> by a simple arithmetic shift. The membranes were recovered after each scaling experiment and prepared for subsequent characterization immediately or stored dry in the refrigerator until the next earliest possibility.

### Scanning electron microscopy (SEM)

Following the pilot plant experiments, the recovered membranes were prepared for surface characterization using SEM. For this, the membranes were cut to approximately 10 mm squares, dried and sputtered with gold at a

current of 40 mA. SEM images were then taken using the Zeiss Supra 55 VP (Carl Zeiss AG, Oberkochen, Germany) at a voltage of 3.00 kV, aperture of 20.00 μm and with the working distance maintained between 5 and 10 mm.

### Biological stability of antiscalants via flow cytometry

The assimilable organic carbon (AOC) analysis was determined by total cell count (TCC) via flow cytometry (CyFlow™ Cube 6 V2m from Sysmex). The AOC reflects the concentration of organic nutrients that are converted during the growth of heterotrophic microorganisms in solution and is considered an important indicator for assessing the re-growth potential and thus the biostability of water. To determine the AOC content, a method was developed by Hammes and Egli<sup>22</sup>, whereby bacterial growth in water samples is observed using flow cytometry. Accordingly, TCC of a sample is tracked for 28 days using flow cytometry measurements carried out on day 0, 3, 7, 14, 21 and 28. On day 0, samples were divided into separate AOC vials for each measurement day (triplicate determination). The samples were then incubated in a shaker incubator at 30 °C and 120 rpm. With the flow cytometer used, all small particles/cells ranging in size from 0.1 μm to 100 μm could be detected and analyzed, with the maximum permitted particle rate being 15,000 events/second. For TCC determination, 1 mL sample solution was prepared in a cuvette: each 100 μL sample was mixed together with 10 μL SYBR® Green I (SG) and 890 μL sterile evian® water. The mixed sample solution was then incubated at 37 °C for 13 min. Both the AOC vials and the cuvettes were well homogenized before each measurement. The instrument was rinsed with the cleaning solution (provided by manufacturer Sysmex) between each sample. Subsequently the AOC content in μg C<sub>eq</sub> L<sup>-1</sup> was calculated using the equation  $\Delta TCC_{\text{flow cytometer}} = TCC_{\text{max}} - TCC_{\text{start}}$  and conversion factor 1·10<sup>7</sup> Cells μg<sup>-1</sup> C from AOC, as given by Hammes and Egli<sup>22</sup> and Vital et al.<sup>23</sup>, respectively. In this study, the antiscalant samples (addition of 1 mg L<sup>-1</sup> TOC by PAA) were prepared in tap water (≈0.5 mg L<sup>-1</sup> TOC before PAA dosing) to provide the bacterial community for AOC analysis. In addition to the antiscalant samples, AOC measurements of the permeate arising from the NF membrane filtration were performed. For this, the lab-scale pilot plant was operated with the flatsheet commercial NF270 membrane, in crossflow mode (crossflow velocity = 0.12 m s<sup>-1</sup>; flux = 62 ± 3 L m<sup>-2</sup> h<sup>-1</sup>) and at a constant TMP of 8 bar.

### Data availability

The datasets used and/or analyzed during the current study available from the corresponding authors on reasonable request.

Received: 9 June 2023; Accepted: 22 April 2024;

Published online: 06 May 2024

### References

- Cohen, Y., Choi, J. Y., Rahardianto, A. Water Reclamation, Remediation, and Cleaner Production with Nanofiltration. In *Nanofiltration*, (eds Schaefer, A. I., Fane, A. G.) 451–497 (Wiley, 2021).
- Matin, A., Rahman, F., Shafi, H. Z. & Zubair, S. M. Scaling of reverse osmosis membranes used in water desalination: Phenomena, impact, and control; future directions. *Desalination* **455**, 135–157 (2019).
- Lin, W., Zhang, Y., Li, D., Wang, X. M. & Huang, X. Roles and performance enhancement of feed spacer in spiral wound membrane modules for water treatment: A 20-year review on research evolution. *Water Res.* **198**, 117146 (2021).
- Yu, W., Song, D., Chen, W. & Yang, H. Antiscalants in RO membrane scaling control. *Water Res.* **183**, 115985 (2020).
- Al-Hamzah, A. A. & Fellows, C. M. A comparative study of novel scale inhibitors with commercial scale inhibitors used in seawater desalination. *Desalination* **359**, 22–25 (2015).
- Zuo et al. Experimental and theoretical studies of carboxylic polymers with low molecular weight as inhibitors for calcium carbonate scale. *Crystals* **10**, 406 (2020).



7. Darton, E. G. Membrane chemical research: centuries apart. *Desalination* **132**, 121–131 (2000).
8. Shen, C., Xu, X., Hou, X. Y., Wu, D. X. & Yin, J. H. Molecular weight effect on PAA antiscalant performance in LT-MED desalination system: Static experiment and MD simulation. *Desalination* **445**, 1–5 (2018).
9. Wang, Y., Li, A. & Yang, H. Effects of substitution degree and molecular weight of carboxymethyl starch on its scale inhibition. *Desalination* **408**, 60–69 (2017).
10. Ali, S. A., Kazi, I. W. & Rahman, F. Synthesis and evaluation of phosphate-free antiscalants to control CaSO<sub>4</sub>·2H<sub>2</sub>O scale formation in reverse osmosis desalination plants. *Desalination* **357**, 36–44 (2015).
11. Yu, W., Wang, Y., Li, A. & Yang, H. Evaluation of the structural morphology of starch-graft-poly (acrylic acid) on its scale-inhibition efficiency. *Water Res.* **141**, 86–95 (2018).
12. Rabizadeh, T., Morgan, D. J., Peacock, C. L. & Benning, L. G. Effectiveness of green additives vs poly (acrylic acid) in inhibiting calcium sulfate dihydrate crystallization. *Ind. Eng. Chem. Res.* **58**, 1561–1569 (2019).
13. Al-Hamzah, A. A., East, C. P., Doherty, W. O. & Fellows, C. M. Inhibition of homogenous formation of calcium carbonate by poly (acrylic acid). The effect of molar mass and end-group functionality. *Desalination* **338**, 93–105 (2014).
14. Armbruster, D., Happel, O. & Egner, S. Charakterisierung und Spurenanalytik technischer Polyacrylate als Antiscalants in der Trinkwasseraufbereitung. *Vom Wasser* **122**, 15–18 (2024).
15. Chong, T. H., Wong, F. S. & Fane, A. G. The effect of imposed flux on biofouling in reverse osmosis: role of concentration polarisation and biofilm enhanced osmotic pressure phenomena. *J. Memb. Sci.* **325**, 840–850 (2008).
16. Vrouwenvelder, J. S. et al. Quantitative biofouling diagnosis in full scale nanofiltration and reverse osmosis installations. *Water Res.* **42**, 4856–4868 (2008).
17. Sweity, A., Oren, Y., Ronen, Z. & Herzberg, M. The influence of antiscalants on biofouling of RO membranes in seawater desalination. *Water Res.* **47**, 3389–3398 (2013).
18. Sweity, A. et al. Side effects of antiscalants on biofouling of reverse osmosis membranes in brackish water desalination. *J. Memb. Sci.* **481**, 172–187 (2015).
19. Ashfaq, M. Y., Al-Ghouti, M. A., Qiblawey, H. & Zouari, N. Evaluating the effect of antiscalants on membrane biofouling using FTIR and multivariate analysis. *Biofouling* **35**, 1–14 (2019).
20. Benecke, J., Rozova, J. & Ernst, M. Anti-scale effects of select organic macromolecules on gypsum bulk and surface crystallization during reverse osmosis desalination. *Sep. Purif. Technol.* **198**, 68–78 (2018).
21. Benecke, J. *Gypsum scaling during reverse osmosis desalination – characterization and effects of natural organic matter*, Doctoral dissertation, Hamburg University of Technology (2018).
22. Hammes, F. A. & Egli, T. New method for assimilable organic carbon determination using flow-cytometric enumeration and a natural microbial consortium as inoculum. *Environ. Sci. Technol.* **39**, 3289–3294 (2005).
23. Vital, M., Fuchslin, H. P., Hammes, F. & Egli, T. Growth of *Vibrio cholerae* O1 Ogawa Eltor in freshwater. *Microbiology* **153**, 1993–2001 (2007).

## Acknowledgements

This study was funded by BMBF (02WAV1530B) and DVGW (W 201807) through the project KonTriSol. Publishing fees supported by Funding Programme Open Access Publishing of Hamburg University of Technology (TUHH). The authors would like to thank Thorsten Dorsch and Jonas Schuster for their assistance with the LC-OCD data and evaluation of microbiology data, respectively. Many thanks to Vikramsheel Singh for contributing to the lab tasks.

## Author contributions

D.A. was responsible for characterization and fractionation of the antiscalants, while S.A.K. mainly designed, carried out and coordinated the effectiveness and bioavailability experiments reported in this trial. M.E. was involved in acquisition, conceptualization and review. J.D. conducted part of the lab experiments, together with D.B-S who carried out some of the flow cytometry measurements and supported data analysis. S.A.K., D.A., B.W. and M.E. contributed to writing and proof-reading the manuscript.

## Funding

Open Access funding enabled and organized by Projekt DEAL.

## Competing interests

The authors declare no competing interests.

## Additional information

**Supplementary information** The online version contains supplementary material available at <https://doi.org/10.1038/s41545-024-00332-7>.

**Correspondence** and requests for materials should be addressed to S. A. Kaushik or M. Ernst.

**Reprints and permissions information** is available at <http://www.nature.com/reprints>

**Publisher's note** Springer Nature remains neutral with regard to jurisdictional claims in published maps and institutional affiliations.

**Open Access** This article is licensed under a Creative Commons Attribution 4.0 International License, which permits use, sharing, adaptation, distribution and reproduction in any medium or format, as long as you give appropriate credit to the original author(s) and the source, provide a link to the Creative Commons licence, and indicate if changes were made. The images or other third party material in this article are included in the article's Creative Commons licence, unless indicated otherwise in a credit line to the material. If material is not included in the article's Creative Commons licence and your intended use is not permitted by statutory regulation or exceeds the permitted use, you will need to obtain permission directly from the copyright holder. To view a copy of this licence, visit <http://creativecommons.org/licenses/by/4.0/>.

© The Author(s) 2024